HHS Public Access

Author manuscript

ACS Nano. Author manuscript; available in PMC 2016 June 20.

Published in final edited form as:

ACS Nano. 2016 January 26; 10(1): 1060–1066. doi:10.1021/acsnano.5b06383.

Dye-Sensitized Core/Active Shell Upconversion Nanoparticles for Optogenetics and Bioimaging Applications

Xiang Wu[†,§,◊], **Yuanwei Zhang**[†,◊], **Kendra Takle**[‡,◊], **Osman Bilsel**[†], **Zhanjun Li**[†], **Hyungseok Lee**[†], **Zijiao Zhang**[⊥], **Dongsheng Li**[#], **Wei Fan**[⊗], **Chunying Duan**[§], **Emory M. Chan**[‖], **Carlos Lois**[‡], **Yang Xiang**[‡], and **Gang Han**[*,†]

[†]Department of Biochemistry and Molecular Pharmacology, University of Massachusetts Medical School, Worcester, Massachusetts 01605, United States

[‡]Neurobiology Department, University of Massachusetts Medical School, Worcester, Massachusetts 01605, United States

[§]State Key Laboratory of Fine Chemicals, Dalian University of Technology, Dalian, 116012, People's Republic of China

[‖]The Molecular Foundry, Lawrence Berkeley National Laboratory, Berkeley, California 94720, United States

[⊥]Department of Materials Science & Engineering, Zhejiang University, Hangzhou, 310027, People's Republic of China

[#]Materials Sciences, Physical and Computational Sciences Directorate, Pacific Northwest National Laboratory, Richland, Washington 99352, United States

[⊗]Chemical Engineering Department, University of Massachusetts, Amherst, Massachusetts 01003, United States

Abstract

Near-infrared (NIR) dye-sensitized upconversion nanoparticles (UCNPs) can broaden the absorption range and boost upconversion efficiency of UCNPs. Here, we achieved significantly enhanced upconversion luminescence in dye-sensitized core/active shell UCNPs via the doping of ytterbium ions (Yb^{3+}) in the UCNP shell, which bridged the energy transfer from the dye to the UCNP core. As a result, we synergized the two most practical upconversion booster effectors (dye-sensitizing and core/shell enhancement) to amplify upconversion efficiency. We demonstrated two biomedical applications using these UCNPs. By using dye-sensitized core/active shell UCNP embedded poly(methyl methacrylate) polymer implantable systems, we successfully shifted the optogenetic neuron excitation window to a biocompatible and deep tissue penetrable

[*]**Corresponding Author:** gang.han@umassmed.edu.

[◊]**Author Contributions**

X. Wu, Y. Zhang, and K. Takle contributed equally to this work.

Supporting Information

The Supporting Information is available free of charge on the ACS Publications website at DOI: 10.1021/acsnano.5b06383. Additional experimental details (PDF)

Notes

The authors declare no competing financial interest.

800 nm wavelength. Furthermore, UCNPs were water-solubilized with Pluronic F127 with high upconversion efficiency and can be imaged in a mouse model.

Graphical abstract

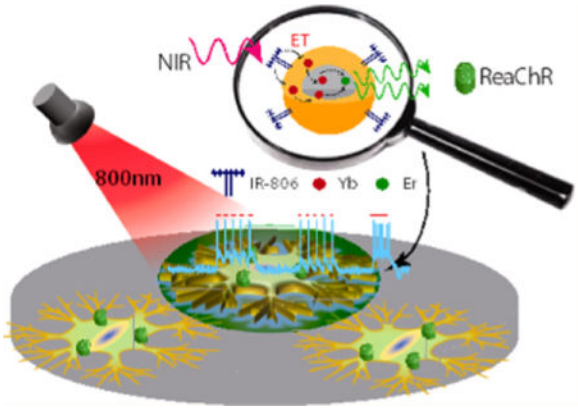

Keywords

bioimaging; core/active shell structure; dye-sensitizing; near-infrared; optogenetics; upconversion nanoparticles

Optogenetic techniques have been developed to control the activities and functions of neurons and to probe the interconnection of neural activities.[1,2] When neural cells are excited by a specific wavelength of light, ion channels that are expressed with microbial opsins after viral transduction or transgenesis can activate or silence neuronal activity.[3] The high spatiotemporal resolution of optogenetic tools has enabled researchers to identify causal relationships between brain activity and behavior. These studies may lead to new therapies for neuropsychiatric diseases. Currently, optogenetic tools rely on visible light that has a shallow depth of tissue penetration, such as ~470 nm for channelrhodopsin-2[3] and ~530 nm for halorhodopsin.[2] In order to deliver visible light into organs and tissues,[4,5] optogenetic protocols typically require the permanent insertion of fiber-optic probes. However, this approach has limitations for chronic stimulation in animals because of potential tissue infections and constraint of the animal with fiber-optic tethers. To address this issue, micro light-emitting diodes (μ-LEDs) have been implanted inside the mouse brain; however, this approach is largely limited by the working distance, replacement, and renewability needs of the energy power source.[6,7] These problems with optogenetics can be addressed by shifting the excitation wavelength to a region with a greater tissue penetration depth and less tissue scattering and blood absorption. For instance, a red-shifted variant of channelrhodopsin (ReaChR) was recently developed that can be excited from 470 to 630 nm.[8] Despite this advance, shifting the optogenetic operation window to the near-infrared (NIR) range (~700–1000 nm) is desirable to allow a deeper light penetration than red light.[9,10]

With recent advances in nanotechnology, lanthanide-doped upconverting nanoparticles (UCNPs) have been developed that can be excited by NIR light and have emissions in the

visible spectrum that can overlap with opsin's activation wavelengths.[11–13] UCNPs are currently used for *in vivo* deep tissue imaging,[14–16] drug delivery,[17,18] photodynamic therapy,[10,19,20] immunotherapy,[21] photoactivation,[22–24] and solar cell development.[25] NIR light at ~800 nm can penetrate transcranially to a depth of at least 4 cm through the human skull, meninges, scalp, and brain.[26] We thus envision the development of UCNPs in an optogenetic application to enhance the penetration of light for activation of neurons.

Despite the considerable potential of UCNPs for diverse applications, there is a need to increase the intensity of upconverting luminescence, as the quantum efficiency of these probes is still suboptimal.[27–29] The following are arguably the two most practical and effective ways to improve UC efficiency. First, utilization of shell growth can synthetically block the surface quenchers to the UCNP core layer.[27,30,31] Second, use of an organic NIR dye can alleviate inherently weak and narrow near-infrared absorption of the lanthanide ions (*e.g.*, Yb^{3+} or Nd^{3+}).[16,32–35] Here, we combine these two strategies to overcome the low quantum efficiency of UCNPs and report the development of dye-sensitized core/active shell upconversion nanoparticles with significantly enhanced upconversion luminescence and a broadened absorption range. Specifically, we doped ytterbium ions into the UCNP shells. As a result, the energy of NIR excitation light peaked at the 800 nm that was absorbed by IR-806 dyes was able to be effectively transferred to the UCNP core *via* doped ytterbium ions in the shells. Further, we demonstrate the proof-of-concept that neurons can be activated by such dye-sensitized core/active shell UCNP embedded poly(methyl methacrylate) (PMMA) matrix when excited at 800 nm. Moreover, these UCNPs were water-solubilized with Pluronic F127 and can be further imaged in a mouse model.

RESULTS AND DISCUSSION

We initially synthesized dye-sensitized core/shell UCNPs using β-$NaYF_4$ shell layers. More specifically, $NaYF_4$:20%Yb, 2%Er core (~20 nm) was used for the epitaxial growth of β-$NaYF_4$ shells with varied thickness (*i.e.*, 2.5, 5, 7.5, 10, and 12.5 nm, respectively) (Figure S1) using a previously reported method.[36] Afterward, we explored the optimal ratio of IR-806 dyes *versus* UCNP cores using a modified method from the literature,[35] and in our study the optimal ratio was determined to be ~60:1 (6 μmol/L:0.1 μmol/L) (Figure S8). We then examined the upconversion emission for the core only and the core/shell UCNPs with IR-806 dye sensitizing under 800 nm continuous wave (CW) laser excitation. As can be seen in Figure 1, the results show that as the thickness of the $NaYF_4$ shell increased, such dye-sensitized core/shell UCNPs decreased in regard to luminescence intensity, reaching nearly its lowest point at a shell thickness of 7.5 nm. This result clearly suggests that a thicker β-$NaYF_4$ shell has an adverse effect on dye-sensitized upconversion emission and that the energy transfer from the IR dye to these UCNPs was blocked due to the increased shell thickness of β-$NaYF_4$. Thus, dye sensitization enhancement could not be extended into core/shell UCNPs with commonly used inert hexagonal-phased β-$NaYF_4$ shells.

Next, we examined the doping of Yb^{3+} ions in the shell. Yb^{3+} ions can relay energy from dyes to the emitters in a core-only UCNP.[35] In addition, in core/active shell UCNP system, Yb^{3+} in the shell can absorb and transfer NIR light (*e.g.*, 980 nm) energy into a UCNP's inner core.[37,38] Here, we envisioned that by doping Yb^{3+} ions in the shell the excitation

energy absorbed by the dyes can be transferred to the shell and then transferred from the shell Yb^{3+} into the core. In this regard, we chose to dope Yb^{3+} into the shell of core/shell UCNPs that had a 7.5 nm thick shell. In doing so, we found that such IR-806 dye-sensitized core/Yb^{3+} active shell nanoparticles (10% Yb^{3+} in the shell layer, *i.e.*, β-$NaYF_4$:20%Yb^{3+}, 2%Er@β-$NaYF_4$:10% Yb^{3+} UCNP) (Figures S3, S13, and S14) exhibited an enhanced upconversion emission under 800 nm excitation. When comparing the integrated upconversion emission area (from 450 to 700 nm), it showed 8 times enhancement in comparison to dye-sensitized core UCNPs (β-$NaYF_4$:20%Yb^{3+}, 2%Er^{3+}) and 70 times greater than the same sized dye-sensitized core/$NaYF_4$ shell UCNP (β-$NaYF_4$:20%Yb^{3+}, 2%Er^{3+}@β-$NaYF_4$) (Figure 2b). Note that IR dyes per UCNP were ~60:1 in the above experiments. In this study, we also varied the Yb^{3+} content (10% Yb^{3+}, 30% Yb^{3+}, and 50% Yb^{3+}) in the shell layer (Figures S3 and S4) and found not only that 10% Yb^{3+} is the optimal doping concentration but that the further increase of Yb^{3+} concentration causes the upconversion intensity to decrease (Figure S11). This decrease is presumably caused by Yb^{3+} cross-relaxation quenching.[37] A controlled experiment of ~20 nm core only β-$NaYF_4$:30%Yb, 2%Er (Figures S5 and S6) was also carried out (*i.e.*, with the same total combined Yb^{3+} concentration as the core/Yb^{3+}-doped shell nanoparticles). The resulting upconversion emission intensity of IR-806-sensitized $NaYF_4$:30%Yb^{3+}, 2%Er^{3+} under 800 nm excitation was also much lower than that of the core/Yb^{3+} shell nanoparticles (Figure S9).

Further, the absolute quantum yield (QY) of our dye-sensitized core/Yb^{3+} shell UCNPs (IR-806-β-$NaYF_4$:20%Yb^{3+}, 2% Er^{3+}@β-$NaYF_4$:10%Yb) in DMF was measured to be ~5% at 2 W/cm^2 of 800 nm. Compared to the current highest value (0.18% at 31 W/cm^2)[39] reported for existing 800 nm excitable UCNPs, our result yields a higher QY at a lower power density.

Moreover, we found that the dye-sensitized core/Yb^{3+}-doped active shell UCNPs have a broadened absorption range. Utilizing this method, the integrated spectral response of the dye-sensitized core/Yb^{3+} shell UCNPs in the wavelength range 720–1000 nm is enhanced ~20-fold when compared to the same UCNPs without dye sensitizing (Figure 3). When compared at a single wavelength of 800 nm, the IR-806-sensitized core/Yb^{3+}-doped active shell shows ~1000 times upconversion luminescence enhancement. Further, when comparing an IR-806-sensitized core/Yb^{3+} active shell UCNP excited at 800 nm to a core-Yb^{3+} active shell UCNP without dye modification that is excited at its optimal wavelength of 980 nm, the IR-806 sensitizion also shows a 7 times enhancement (Figures 3 and S12). This result shows that the upconversion luminescence of UCNPs can be effectively enhanced by using organic dye molecules as the sensitizer in a core/active shell structure.

Since we are now able to combine the two best strategies to significantly improve upconversion efficiency, we envision that these dye-sensitized core/Yb^{3+} active shell UCNPs can address the limitation of poor tissue penetration depth of current optogenetic tools. As an initial proof-of-principle, we set out to develop an implantable device to test whether our UCNP systems can function as a relay for NIR light in regard to the activation of optogenetic constructs in neuronal cells. We encapsulated our dye-sensitized core/Yb^{3+} active shell UCNPs into PMMA polymers so as to fabricate a thin film. We found that this

film is resistant to water quenching in PBS buffer (Figure S17). This film was then placed directly beneath a glass coverslip containing cultured hippocampal neurons. Red light activatable channelrhodopsin revealed consistent depolarization and the act of potential firing in response to the light whose wavelength overlaps with the emission of dye-sensitized core/Yb^{3+} shell UCNPs[8] (Figure S15). Notably, in our study, when 800 nm NIR light was delivered in order to stimulate neurons, we observed robust neuronal activation in a light intensity-dependent manner (Figure 4). Neuronal depolarization depends on the intensity of the NIR (Figure 4c), and the threshold intensities for significant depolarization and the act of potential firing are 0.117 and 1.5 W/mm^2, respectively (Figure 4c and d). These power densities are about two to three magnitudes lower than what is currently used in two-photon technology for neuron cell activation (*e.g.*, 1×10^5 W/cm^2 [40] or 4.5×10^4 W/cm^2 [41]). Importantly, the UCNP system allows for precise temporal control of neuronal activation, as neuronal action potential was able to follow patterns of light pulses (*e.g.*, 100 ms, 500 ms, 2 s) in a time-locked fashion (Figure 4b). Next, to control for possible thermal and other potential side effects that are associated with NIR light delivery, we tested cultured hippocampal neurons in the following ways: without the UCNPs, without the ReaChR transfection, or with core/Yb^{3+} active shell UCNPs in absence of core Er^{3+} ion doping (~35 nm β-$NaYF_4$:20%Yb^{3+} @β-$NaYF_4$, 10%Yb^{3+}) (Figure S7) where NIR absorption does not generate the emission of visible light under 800 nm excitation (Figure S10). In all three sets of control experiments, we found a great deal of reduced neuronal depolarization and the act of potential firing compared to the conditions that included opsin and our dye-sensitized core/Yb^{3+} active shell UCNPs (Figure 4c). It is noteworthy that we noticed that NIR light at high intensities (*i.e.*, 4.29 W/mm^2) does, in rare cases, activate the neuron (Figure 4d). Our results clearly demonstrate that NIR light at 800 nm is able to activate optogenetic constructs in order to manipulate neuronal activities. Moreover, optogenetic applications rely on pulsed light delivery compared to long exposure times with other application realms using upconversion nanoparticles (for example, photouncage[23]). We have observed that quite a short duration laser exposure (*i.e.*, 100 ms) can trigger neuron cell action potential firing.

Furthermore, we also water-solubilized our dye-sensitized core/active shell UCNPs (IR806-β-$NaYF_4$:20%Yb^{3+}, 2%Er^{3+}@β-$NaYF_4$, 10%Yb^{3+}) for bioimaging applications. Hydrophobic dye-sensitized core/Yb^{3+} active shell UCNPs were rendered water-soluble *via* wrapping them in the amphiphilic triblock copolymer Pluronic F127.[42,43] The resultant triblock copolymer micelle possessed a hydrophobic core to encapsulate the hydrophobic oleic acid ligand coated UCNPs through van der Waal's force. It also has a hydrophilic shell, offering it aqueous stability (Figure 5). The as-synthesized micelles were able to disperse in aqueous solution with an average hydrodynamic size of ~110 nm in water. In PBS, the resulting micelle encapsulation has an average particle size that is similar to that in pure water (Figure S19). After micelle encapsulation, the luminescence of these UCNPs can be visualized by the naked eye (Figure 5b inset). Its upconversion luminescence remained above 30% under 2 W/cm^2 of 800 nm laser (Figure 5b). It is noteworthy that we noticed that there was a certain luminescence decrease over 10 min (Figure S16). The *in vivo* animal imaging study of such micelle-encapsulated dye-sensitized UCNPs was evaluated *via* the use of a Maestro EX small-animal optical imaging system. Following subcutaneous administration of micelle-encapsulated dye-sensitized core/Yb^{3+} shell UCNPs, we observed

clear UCNP characteristic luminescent signals *in vivo* under 800 nm excitation (Figure S20). This suggests the feasibility of biophotonic application for dye-sensitized core/Yb^{3+} active shell UCNPs.

CONCLUSIONS

In conclusion, we synergized two state-of-the-art approaches for the enhancement of upconversion efficiency and were able to demonstrate dye-sensitized core/Yb^{3+} active shell UCNPs with broadened absorption and elevated upconversion efficiency. We doped Yb^{3+} ions in the shell in order to bridge the energy transfer from the NIR dye to UCNP core, the latter of which is otherwise blocked by the commonly used core/$NaYF_4$ shell UCNPs. These dye-sensitized UCNPs were further applied for optogenetic analysis in the NIR tissue optical window for potential use in controlling neuronal activity. We further water-solubilized these UCNPs and demonstrated their use for bioimaging applications. We offer an interesting strategy to improve the upconversion efficiency of UCNPs, which will pave the way for new biological and medical applications.

MATERIALS AND METHODS

General Chemicals

IR-780 iodide (99%), 4-mercaptobenzoic acid (99%), Y_2O_3 (99.9%), Yb_2O_3 (99.9%), Er_2O_3 (99.9%), CF_3COONa (99.9%), CF_3COOH, 1-octadecene (90%), oleic acid (90%), oleylamine (90%), *N*,*N*-dimethylformamide (DMF, anhydrous, 99.8%), and dichloromethane (DCM, AR grade) were all purchased from Sigma-Aldrich and used without further purification. The lanthanide (Ln) trifluoroacetates, $Ln(CF_3COO)_3$, were prepared as described in the literature.[10]

Instrumentation

^1H NMR spectra were recorded on a Varian AMX400 (400 MHz) using d_6-DMSO as solvent at room temperature. Transmission electron microscopy (TEM) was performed on a Philips CM10 transmission electron microscope operating at an accelerating voltage of 100 kV. Images were recorded on a Gatan slow-scan CCD camera. The powder X-ray diffraction (XRD) patterns were recorded by a Vantec-500 area detector using Co Kα radiation (1.79 Å). The 2θ angle of the XRD spectra was recorded at a scanning rate of 5 deg/min and then was converted to Cu Kα radiation values by Bragg's law. The size distribution of the samples was determined by dynamic light scattering (DLS) equipped with a Zetasizer Nano-ZS (He–Ne laser wavelength at 633 nm) and an autotitrator (Malvern Instruments, Malvern, UK). The upconversion photoluminescence emission spectrum was measured using a fluorospectrophotometer (Fluorolog-3, HORIBA, USA). The samples were excited by either a 980 or 800 nm continuous wave laser under the power density of 2 W/cm^2 (Hi-Tech Optoelectronics Co., Ltd., China). BALB/c mice (female, 4–8 weeks, from Jackson Laboratory) were used for the imaging experiment. Hair on the back of the mice was shaved, and the mice were anesthetized using iv-injected ketamine/xylazine during imaging (Maestro EX system). Micelle-encapsulated dye-sensitized UCNPs (200 μL, 10 mg/mL) were injected subcutaneously 10 min before imaging (800 nm CW laser excitation, 1 W/

cm^2, 1 s exposure time). The animal procedures were approved by the University of Massachusetts Medical School Institutional Animal Care and Use Committee. The NIR photoluminescence emission spectrum of IR-806 dye was measured with excitation at 750 nm and emission measured from 775 to 1200 nm using a Horiba Nanolog spectrofluorometer with a 5509 PMT detector and 450 W xenon lamp. For the upconversion excitation spectrum measurements, the Ti:sapphire laser was switched to continuous-wave mode, and the absence of mode-locking was confirmed by monitoring the laser output using a 400 MHz oscilloscope and fast photodiode. The detection utilized a bandpass filter (FF01-524/24-25, Semrock, Rochester, NY, USA) and a PMH100-6 photomultiplier tube module from Becker-Hickl. A pulse generator provided a 5 MHz sync signal to the TCSPC electronics, and the photons over the time-to-amplitude converter range were integrated to provide the total signal for each excitation wavelength. In order to use a constant excitation intensity (2 mW) at each wavelength, a 1 mm thick quartz plate was used to pick off part of the excitation beam and direct it to a calibrated power meter (corrected for the excitation wavelengths, Newport 1830-C with 818 series detector).

Synthetic Procedures

The synthesis of IR-806—The IR-806 was synthesized the same as the method described in the literature.

Synthesis of β-$NaYF_4$:20%Yb, 2%Er Core UCNPs, β-$NaYF_4$:20%Yb Core UCNPs, and β-$NaYF_4$:30%Yb, 2%Er UCNPs—Synthesis of *β*-$NaYF_4$:Ln core UCNPs: The *β*-$NaYF_4$:Ln core UCNPs were prepared by a two-step thermolysis method. In the first step, CF_3COONa (0.5 mmol) and proper $Ln(CF_3COO)_3$ ((Y+Yb+Er) 0.5 mmol in total; for *β*-$NaYF_4$:20%Yb, 2%Er, Y:Yb:Er = 78%:20%:2%; for *β*-$NaYF_4$:20%Yb, Y:Yb = 80%:20%; for *β*-$NaYF_4$:30%Yb, 2%Er, Y:Yb:Er = 68%:30%:2%) precursors were mixed with oleic acid (5 mmol), oleyamine (5 mmol), and 1-octadecene (10 mmol) in a two-neck reaction flask. The slurry mixture was heated to 110 °C to form a transparent solution followed by 10 min of degassing. Then the flask was heated to 300 °C at a rate of 15 °C/min under dry argon flow, and it was maintained at 300 °C for 30 min. The *α*-$NaYF_4$:Ln intermediate UCNPs were gathered from the cooled reaction solution by centrifugal washing with excessive ethanol (7500*g*, 30 min). In the second step, the *α*-$NaYF_4$:Ln intermediate UCNPs were redispersed into oleic acid (10 mmol) and 1-octadecene (10 mmol) together with CF_3COONa (0.5 mmol) in a new two-neck flask. After degassing at 110 °C for 10 min, this flask was heated to 325 °C at a rate of 15 °C/min under dry argon flow, and it remained at 325 °C for 30 min. Then, *β*-$NaYF_4$:Ln UCNPs were centrifugally separated from the cooled reaction media and preserved in hexane (10 mL) as stock solution.

Synthesis of Core/$NaYF_4$ Shell and Core/Yb^{3+}-Doped Shell UCNPs—In this thermolysis reaction, as-synthesized 20 nm *β*-$NaYF_4$:20%Yb, 2%Er UCNPs or *β*-$NaYF_4$:20%Yb (for the synthesis of ~35 nm *β*-$NaYF_4$:20%Yb/*β*-$NaYF_4$:10%Yb control core/shell) served as cores for the epitaxial growth of undoped *β*-$NaYF_4$ shells and Yb^{3+}-doped shells. Typically, a stock solution of *β*-$NaYF_4$:20%Yb, 2% Er UCNPs (5 mL, *ca.* 1 *μ*mol/L core UCNPs) was transferred into a two-neck flask, and hexane was sequentially removed by heating. To prepare core/$NaYF_4$ shell *β*-$NaYF_4$:20%Yb, 2%Er/*β*-$NaYF_4$ UCNPs

with increased shell thickness, increasing amounts of CF_3COONa (0.1, 0.25, 0.5, 0.75, and 1 mmol) and $Y(CF_3COO)_3$ (0.1, 0.25, 0.5, 0.75, and 1 mmol) were used, respectively. To prepare ~35 nm core/Yb^{3+} shell UCNPs, CF_3COONa (0.5 mmol) and $Ln(Y+Yb)(CF_3COO)_3$ (0.5 mmol) were used, The mole percentages of $Y(CF_3COO)_3$ of 90%, 70%, and 50% and $Yb(CF_3COO)_3$ of 10%, 30%, and 50% were used. In these reactions, the above-mentioned precursors were introduced as UCNP shell precursors with oleic acid (10 mmol) and 1-octadecene (10 mmol). After 10 min of degassing at 110 °C, the flask was heated to 325 °C at a rate of 15 °C/min under dry argon flow and was kept at 325 °C for 30 min. The products were precipitated by adding 20 mL of ethanol to the cooled reaction flask. After centrifugal washing with hexane/ethanol (7500*g*, 30 min), the core/shell UCNPs were redispersed in 10 mL of hexane.

Dye-Sensitized Upconversion Nanoparticle Preparation—IR-806 dye-sensitized UCNPs were prepared based on a modified literature method. More specifically, they were prepared by mixing different amounts of IR-806 into UCNPs in DCM/hexane (v/v 1:10). The final concentrations of UCNPs are 0.1 μmol/L; the final concentrations of IR-806 are 0, 2, 4, 6, 25, 50, and 100 μmol/L. All the solutions mentioned above stood for 1 h at room temperature before measurements. The dye-conjugated core/shell UCNPs can be isolated by centrifugation (12000*g*, 30 min) and can be redissolved in DMF.

Fabrication of UCNP-Encapsulated PMMA Film—IR-806 and 35 nm *β*-$NaYF_4$:20%Yb, 2% Er/*β*-$NaYF_4$:10%Yb core/Yb active shell UCNPs (0.06 mmol:1 μmol) were first mixed in DCM/hexane (1 mL, 1:10, v/v). After 1 h of continuous stirring, the dye-conjugated core/shell UCNPs were isolated by centrifugation. The dye-coated nanoparticles were redissolved in a small amount of DMF. Meanwhile, 200 mg of PMMA was dissolved in 1 mL of DMF at 100 °C. This was then cooled to room temperature. Then a dye-conjugated UCNP DMF solution was blended with the above prepared PMMA. The resulting mixture was pasted onto a cover glass and remained overnight at room temperature to obtain a transparent PMMA thin film that includes dye-sensitized core/Yb^{3+} active shell UCNPs. Control samples were prepared using the same amount of reagents with IR dye only or with dye-modified ~35 nm (20 nm core and 7.5 nm shell) *β*-$NaYF_4$:20%Yb/*β*-$NaYF_4$, 10%Yb UCNPs (*i.e.*, in the absence of Er^{3+} emitters).

Micelle Encapsulation

A 2 mg amount of dye-coated core/Yb^{3+} shell UCNPs in 0.2 mL of hexane/DCM (10:1, v/v) was slowly added into 2 mL of a Pluronic F-127 aqueous solution (0.5%, w/v). Under vigorous stirring conditions, the organic solvent was allowed to slowly evaporate at room temperature for 4 h. Micelle-encapsulated dye-sensitized UCNPs were collected *via* centrifugation at 12000*g* at a temperature below 4 °C for 30 min.

Electrophysiology

Whole-cell patch clamp recordings of the neurons virally infected with red activatable channelrhodopsin and red fluorescent protein (RFP) were performed 2–3 weeks after plating on an upright microscope with a 40× (NA 1.0) water immersion lens. The 800 nm CW laser was delivered at increasing intensities through the objective. Neurons growing on glass

coverslips were removed from the culture dish and placed in external saline solution composed of (in mM) NaCl 125, KCl 2.5, NaH_2PO_4 1.25, $MgCl_2$ 1, $CaCl_2$ 2, $NaHCO_3$ 26, glucose 20. The osmolality was 312 mOsm kg^{-1}, and the pH was 7.3. RFP-positive neurons were located under a Zeiss D1 microscope with a 40×/1.0 NA water immersion objective lens. Neurons were recorded with a recording pipet (5 μm tip opening) filled with internal saline solution composed of (in mM) potassium gluconate 120, KCl 10, HEPES 10, MgATP 4, NaGTP 0.3, Na phosphocreatine·H_2O 5, EGTA 0.2, pH 7.3, OSM 290 mM. Recordings were performed with a 700B amplifier (Molecular Devices), and the data were acquired with Digidata 1440A (Molecular Devices) and Clampex 10.6 software (Molecular Devices). Electrophysiological recordings of action potentials were obtained in current clamp mode with current injection to sustain −65 mV at rest. A 2 kHz low-pass filter and a sampling frequency of 20 kHz were used. Only excitable cells with a membrane resistance of >200 MΩ and with action potential firing upon green light exposure (except for nontransfected controls) were analyzed. After each recording sweep, we injected a hyperpolarizing current to measure passive membrane properties. Any cell with >10% change during the recording was discarded.

Neuronal Culture

All experiments were approved by the local Animal Welfare Committee. Embryonic day 17 hippocampi from Sprague-Drawley rats were dissected in Hank's balanced salt solution (Invitrogen) containing $MgCl_2$ and Hepes (Sigma) and digested with papain (Worthington). Papain was inactivated by ovomucoid (Worthington), and the tissue was dissociated in culture medium [neurobasal medium containing B27 supplement, penicillin, streptomycin, and glutamine (Invitrogen)]. Cells were infected with a self-inactivating lentiviral vector in which the RSV promoter drives expression of ReacHR fused to the red fluorescent protein mcherry. The lentiviral vector was prepared, concentrated, and titrated. Dissociated neurons were incubated for 1 h at 37 °C in suspension with the lentiviral vector at a multiplicity of infection of 1:1 (1 viral particle per 1 neuron) and plated at a density of 150 000 cells per milliliter of medium on coverslips coated with poly-D-lysine (Sigma) and laminin (Invitrogen). Culture medium was exchanged after 24 h and subsequently changed twice a week. Neurons were recorded after 14 days *in vitro*.

Absolute Quantum Yield Measurement

This testing was done at the Molecular Foundry, a User Facility of the U.S. Department of Energy. A cylindrical quartz cuvette was loaded with 500 μL of a freshly prepared solution of dye-conjugated nanoparticles (0.01 μmol/L). The cuvette was placed in a calibrated integrating sphere coupled with fiber-optics to a Horiba Jobin Yvon Fluorolog-3 spectrometer. Samples were excited with an 800 nm laser (2 W/cm^2, Hi-Tech Optoelectronics), and emission spectra (450–720 nm) and spectra of scattered excitation light (797–804 nm) of the samples and the solvent blank were recorded. All spectra were corrected for the wavelength-dependent sensitivity of the apparatus. The absolute quantum yield of each sample was determined according to the equation $QY = (I_{em,sample} - I_{em,blank})/(I_{ex,blank} - I_{ex,sample})$. Here, I_x is the integrated intensity of the emission (em) or scattering (ex) spectrum for the sample or blank (x).

Supplementary Material

Refer to Web version on PubMed Central for supplementary material.

Acknowledgments

This research was supported by the China Scholarship Council (CSC) to X.W., a Worcester Foundation Mel Cutler Award, National Institutes of Health R01MH103133 to G.H, C.L., and Y.X., Human Frontier Science Program RGY-0090/2014 to G.H. and Y.X. Quantum yield work (E.M.C.) at the Molecular Foundry was supported by the U.S. Department of Energy under Contract No. DE-AC02-05CH11231. D.L. is supported by the U.S. Department of Energy, Office of Science, Office of Basic Energy Sciences Early Career Research Program, under Award No. 67037. We also thank Dr. Shaul Aloni's help in TEM measurements.

References

1. Fenno L, Yizhar O, Deisseroth K. The Development and Application of Optogenetics. Annu Rev Neurosci. 2011; 34:389–412. [PubMed: 21692661]
2. Zhang F, Wang LP, Brauner M, Liewald JF, Kay K, Watzke N, Wood PG, Bamberg E, Nagel G, Gottschalk A, Deisseroth K. Multimodal Fast Optical Interrogation of Neural Circuitry. Nature. 2007; 446:633–U4. [PubMed: 17410168]
3. Boyden ES, Zhang F, Bamberg E, Nagel G, Deisseroth K. Millisecond-Timescale, Genetically Targeted Optical Control of Neural Activity. Nat Neurosci. 2005; 8:1263–1268. [PubMed: 16116447]
4. Grill WM, Norman SE, Bellamkonda RV. Implanted Neural Interfaces: Biochallenges and Engineered Solutions. Annu Rev Biomed Eng. 2009; 11:1–24. [PubMed: 19400710]
5. Huang H, Delikanli S, Zeng H, Ferkey DM, Pralle A. Remote Control of Ion Channels and Neurons Through Magnetic-Field Heating of Nanoparticles. Nat Nanotechnol. 2010; 5:602–606. [PubMed: 20581833]
6. McCall JG, Kim TI, Shin G, Huang X, Jung YH, Al-Hasani R, Omenetto FG, Bruchas MR, Rogers JA. Fabrication and Application of Flexible, Multimodal Light-Emitting Devices for Wireless Optogenetics. Nat Protoc. 2013; 8:2413–2428. [PubMed: 24202555]
7. Kim TI, McCall JG, Jung YH, Huang X, Siuda ER, Li YH, Song JZ, Song YM, Pao HA, Kim RH, Lu C, Lee SD, Song IS, Shin G, Al-Hasani R, Kim S, Tan MP, Huang Y, Omenetto FG, Rodger JA, et al. Injectable, Cellular-Scale Optoelectronics with Applications for Wireless Optogenetics. Science. 2013; 340:211–216. [PubMed: 23580530]
8. Lin JY, Knutsen PM, Muller A, Kleinfeld D, Tsien RY. ReaChR: A Red-Shifted Variant of Channelrhodopsin Enables Deep Transcranial Optogenetic Excitation. Nat Neurosci. 2013; 16:1499–1508. [PubMed: 23995068]
9. Kam NWS, O'Connell M, Wisdom JA, Dai HJ. Carbon Nanotubes as Multifunctional Biological Transporters and Near-Infrared Agents for Selective Cancer Cell Destruction. Proc Natl Acad Sci USA. 2005; 102:11600–11605. [PubMed: 16087878]
10. Punjabi A, Wu X, Tokatli-Apollon A, El-Rifai M, Lee H, Zhang YW, Wang C, Liu Z, Chan EM, Duan CY, Han G. Amplifying the Red-Emission of Upconverting Nanoparticles for Biocompatible Clinically Used Prodrug-Induced Photodynamic Therapy. ACS Nano. 2014; 8:10621–10630. [PubMed: 25291544]
11. Haase M, Schafer H. Upconverting Nanoparticles. Angew Chem, Int Ed. 2011; 50:5808–5829.
12. Zhou J, Liu Z, Li FY. Upconversion Nanophosphors for Small-Animal Imaging. Chem Soc Rev. 2012; 41:1323–1349. [PubMed: 22008740]
13. Wang F, Liu XG. Recent Advances in the Chemistry of Lanthanide-Doped Upconversion Nanocrystals. Chem Soc Rev. 2009; 38:976–989. [PubMed: 19421576]
14. Liu Q, Sun Y, Yang TS, Feng W, Li CG, Li FY. Sub-10 nm Hexagonal Lanthanide-Doped $NaLuF_4$ Upconversion Nanocrystals for Sensitive Bioimaging *In Vivo*. J Am Chem Soc. 2011; 133:17122–17125. [PubMed: 21957992]

15. Chen GY, Shen J, Ohulchanskyy TY, Patel NJ, Kutikov A, Li ZP, Song J, Pandey RK, Agren H, Prasad PN, Han G. Alpha-$NaYbF_4$:Tm^{3+})/CaF_2 Core/Shell Nanoparticles with Efficient Near-Infrared to Near-Infrared Upconversion for High-Contrast Deep Tissue Bioimaging. ACS Nano. 2012; 6:8280–8287. [PubMed: 22928629]
16. Wu X, Chen G, Shen J, Li Z, Zhang Y, Han G. Upconversion Nanoparticles: A Versatile Solution to Multiscale Biological Imaging. Bioconjugate Chem. 2015; 26:166–175.
17. Yang DM, Ma PA, Hou ZY, Cheng ZY, Li CX, Lin J. Current Advances in Lanthanide Ion (Ln^{3+})-Based Upconversion Nanomaterials for Drug Delivery. Chem Soc Rev. 2015; 44:1416–1448. [PubMed: 24988288]
18. Shen J, Zhao L, Han G. Lanthanide-Doped Upconverting Luminescent Nanoparticle Platforms for Optical Imaging-Guided Drug Delivery and Therapy. Adv Drug Delivery Rev. 2013; 65:744–755.
19. Idris NM, Jayakumar MKG, Bansal A, Zhang Y. Upconversion Nanoparticles AsVersatile Light Nanotransducers for Photoactivation Applications. Chem Soc Rev. 2015; 44:1449–1478. [PubMed: 24969662]
20. Chen Q, Wang C, Cheng L, He WW, Cheng Z, Liu Z. Protein Modified Upconversion Nanoparticles for Imaging-Guided Combined Photothermal and Photodynamic Therapy. Biomaterials. 2014; 35:2915–2923. [PubMed: 24412081]
21. Xiang J, Xu LG, Gong H, Zhu WW, Wang C, Xu J, Feng LZ, Cheng L, Peng R, Liu Z. Antigen-Loaded Upconversion Nanoparticles for Dendritic Cell Stimulation, Tracking, and Vaccination in Dendritic Cell-Based Immunotherapy. ACS Nano. 2015; 9:6401–6411. [PubMed: 26028363]
22. Jayakumar MKG, Idris NM, Zhang Y. Remote Activation of Biomolecules in Deep Tissues Using Near-Infrared-to-UV Upconversion Nanotransducers. Proc Natl Acad Sci USA. 2012; 109:8483–8488. [PubMed: 22582171]
23. Yang YM, Shao Q, Deng RR, Wang C, Teng X, Cheng K, Cheng Z, Huang L, Liu Z, Liu XG, Xing BG. *In Vitro* and *In Vivo* Uncaging and Bioluminescence Imaging by Using Photocaged Upconversion Nanoparticles. Angew Chem, Int Ed. 2012; 51:3125–3129.
24. Shen J, Chen G, Ohulchanskyy TY, Kesseli SJ, Buchholz S, Li Z, Prasad PN, Han G. Tunable Near Infrared to Ultraviolet Upconversion Luminescence Enhancement in (Alpha-$NaYF_4$:Yb,Tm)/CaF_2 Core/Shell Nanoparticles for In Situ Real-Time Recorded Biocompatible Photoactivation. Small. 2013; 9:3213–3217. [PubMed: 23696330]
25. Wang HQ, Batentschuk M, Osvet A, Pinna L, Brabec CJ. Rare-Earth Ion Doped Up-Conversion Materials for Photovoltaic Applications. Adv Mater. 2011; 23:2675–2680. [PubMed: 21823249]
26. Tedford CE, DeLapp S, Jacques S, Anders J. Quantitative Analysis of Transcranial and Intraparenchymal Light Penetration in Human Cadaver Brain Tissue. Lasers Surg Med. 2015; 47:312–322. [PubMed: 25772014]
27. Han SY, Deng RR, Xie XJ, Liu XG. Enhancing Luminescence in Lanthanide-Doped Upconversion Nanoparticles. Angew Chem, Int Ed. 2014; 53:11702–11715.
28. Chen GY, Han G. Theranostic Upconversion Nanoparticles (I). Theranostics. 2013; 3:289–291. [PubMed: 23606916]
29. Chan EM, Levy ES, Cohen BE. Rationally Designed Energy Transfer in Upconverting Nanoparticles. Adv Mater. 2015; 27:5753–5761. [PubMed: 25809982]
30. Chen X, Peng D, Ju Q, Wang F. Photon Upconversion in Core-Shell Nanoparticles. Chem Soc Rev. 2015; 44:1318–1330. [PubMed: 25058157]
31. Wang F, Wang J, Liu X. Direct Evidence of a Surface Quenching Effect on Size-Dependent Luminescence of Upconversion Nanoparticles. Angew Chem, Int Ed. 2010; 49:7456–7460.
32. Shen J, Chen GY, Vu AM, Fan W, Bilsel OS, Chang CC, Han G. Engineering the Upconversion Nanoparticle Excitation Wavelength: Cascade Sensitization of Tri-doped Upconversion Colloidal Nanoparticles at 800 nm. Adv Opt Mater. 2013; 1(9):644–650.
33. Wang YF, Liu GY, Sun LD, Xiao JW, Zhou JC, Yan CH. Nd^{3+}-Sensitized Upconversion Nanophosphors: Efficient *In Vivo* Bioimaging Probes with Minimized Heating Effect. ACS Nano. 2013; 7:7200–7206. [PubMed: 23869772]
34. Xie X, Liu X. Photonics: Upconversion Goes Broadband. Nat Mater. 2012; 11:842–843. [PubMed: 23001234]

35. Zou WQ, Visser C, Maduro JA, Pshenichnikov MS, Hummelen JC. Broadband Dye-Sensitized Upconversion of Near-Infrared Light. Nat Photonics. 2012; 6:560–564.

36. Mai HX, Zhang YW, Si R, Yan ZG, Sun LD, You LP, Yan CH. High-Quality Sodium Rare-Earth Fluoride Nanocrystals: Controlled Synthesis and Optical Properties. J Am Chem Soc. 2006; 128:6426–6436. [PubMed: 16683808]

37. Vetrone F, Naccache R, Mahalingam V, Morgan CG, Capobianco JA. The Active-Core/Active-Shell Approach: A Strategy to Enhance the Upconversion Luminescence in Lanthanide-Doped Nanoparticles. Adv Funct Mater. 2009; 19:2924–2929.

38. Yang DM, Li CX, Li GG, Shang MM, Kang XJ, Lin J. Colloidal Synthesis and Remarkable Enhancement of the Upconversion Luminescence of $BaGdF_5:Yb^{3+}/Er^{3+}$ Nanoparticles by Active-Shell Modification. J Mater Chem. 2011; 21:5923–5927.

39. Liu B, Chen Y, Li C, He F, Hou Z, Huang S, Zhu H, Chen X, Lin J. Poly(Acrylic Acid) Modification of Nd^{3+}-Sensitized Upconversion Nanophosphors for Highly Efficient UCL Imaging and pH-Responsive Drug Delivery. Adv Funct Mater. 2015; 25:4717–4729.

40. Mohanty SK, Reinscheid RK, Liu X, Okamura N, Krasieva TB, Berns MW. In-Depth Activation of Channelrhodopsin 2-Sensitized Excitable Cells with High Spatial Resolution Using Two-Photon Excitation with a Near-Infrared Laser Microbeam. Biophys J. 2008; 95:3916–3926. [PubMed: 18621808]

41. Papagiakoumou E, Anselmi F, Begue A, de Sars V, Gluckstad J, Isacoff EY, Emiliani V. Scanless Two-Photon Excitation of Channelrhodopsin-2. Nat Methods. 2010; 7:848–854. [PubMed: 20852649]

42. Basak R, Bandyopadhyay R. Encapsulation of Hydrophobic Drugs in Pluronic F127 Micelles: Effects of Drug Hydrophobicity, Solution Temperature, and pH. Langmuir. 2013; 29:4350–4356. [PubMed: 23472840]

43. Liu L, Yong KT, Roy I, Law WC, Ye L, Liu J, Kumar R, Zhang X, Prasad PN. Bioconjugated Pluronic Triblock-Copolymer Micelle-Encapsulated Quantum Dots for Targeted Imaging of Cancer: *in vitro* and *in vivo* Studies. Theranostics. 2012; 2:705–713. [PubMed: 22896772]

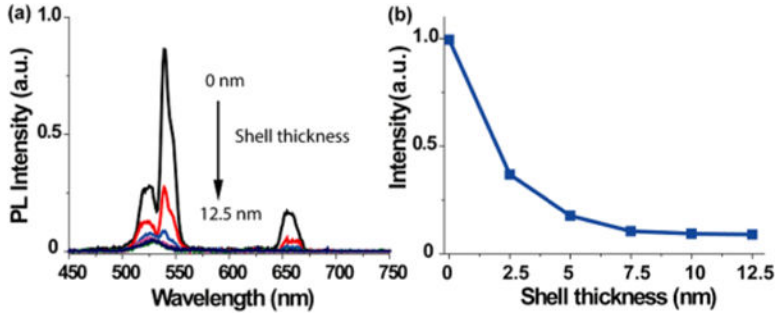

Figure 1.

(a) Emission spectra of IR-806-dye-senstized UCNPs exhibiting various β-$NaYF_4$ shell thickness (i.e., 0, 2.5, 5, 7.5, 10, and 12.5 nm, respectively) upon 800 nm CW laser excitation. (b) The integrated emission peak area (from 500 to 700 nm) of those dye-sensitized UCNPs decreases as the shell thickness increases. Note: In order to guide the eye, the data points are connected by lines.

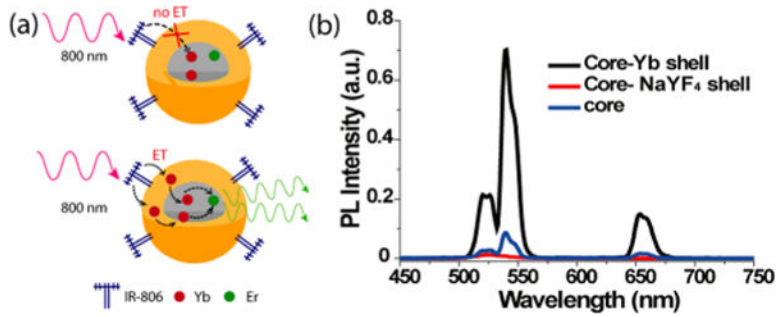

Figure 2.

(a) Schematic showing the proposed energy transfer mechanism for core/shell UCNPs without (top) and with (bottom) Yb^{3+} doping. (b) Emission spectra of IR-806-sensitized core only (β-$NaYF_4$:20%Yb^{3+}, 2%Er^{3+}), core/$NaYF_4$ shell (β-$NaYF_4$:20%Yb^{3+}, 2%Er^{3+}@β-$NaYF_4$), core/Yb^{3+} shell (β-$NaYF_4$:20%Yb^{3+}, 2%Er^{3+}@β-$NaYF_4$:10%Yb^{3+}). Note: The shell exhibited a controlled thickness of ~7.5 nm for core/$NaYF_4$ shell and core/Yb^{3+} shell UCNPs. The measurements were performed under 800 nm continuous wave laser excitation (2 W/cm^2), with a UCNP concentration of 0.1 μmol/L (ET: energy transfer).

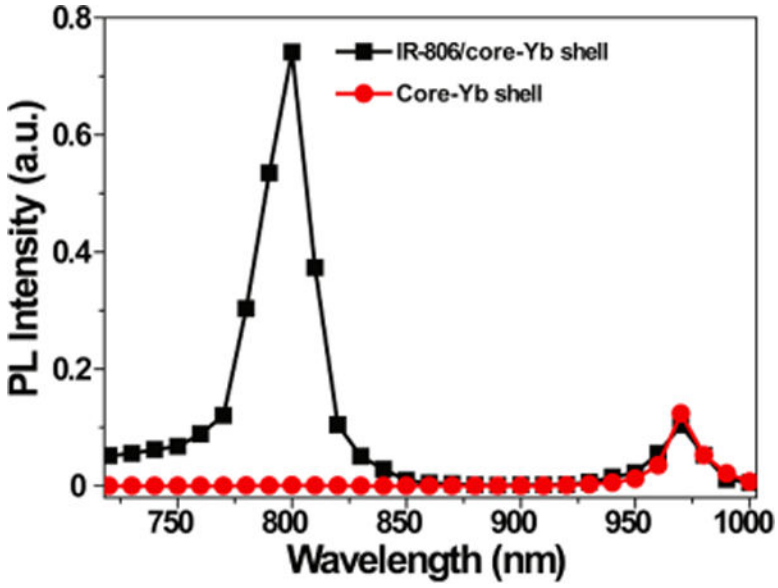

Figure 3.

Excitation spectrum of β-$NaYF_4$:20%Yb^{3+}, 2%Er^{3+}@β-$NaYF_4$:10%Yb^{3+} (core/Yb^{3+} active shell) nanoparticle with (black squares) and without (red circles) IR-806 dye sensitization.

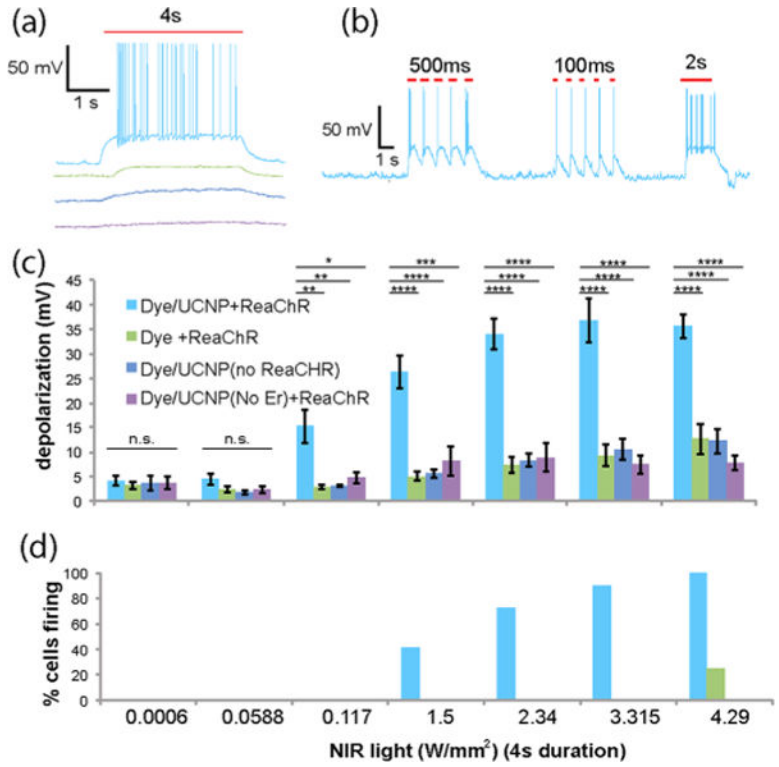

Figure 4.

Near infrared light activation of ReaChR in cultured hippocampal neurons. Examples of the act of potential firing in response to (a) prolonged (4 s) and (b) pulsed (100 ms, 500 ms, 2 s) delivery of 800 nm NIR light (2.34 W/mm^2). (c) Neuronal depolarization and (d) firing triggered by 800 nm NIR light at different intensities for a duration of 4 s. Note that there can be depolarization and neuronal activation even in some control cases. **, $p < 0.01$, ****, $p < 0.0001$. One-way ANOVA with Bonferroni correction. The four color squares in (c) are annotations for (a)–(d).

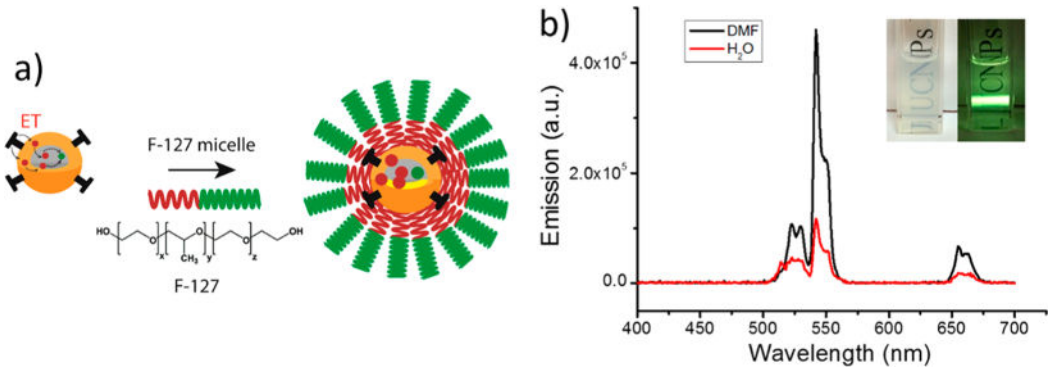

Figure 5.

(a) Schematic of the phase transfer procedure using Pluronic F-127 as encapsulation material. (b) Emission spectra of dye-sensitized core/Yb^{3+} shell UCNPs (1 mg/mL) before micelle encapsulation in DMF (black curve) and after encapsulation in PBS (red curve), acquired upon 800 nm CW laser excitation (2 W/cm^2). The inset displays photographs of micelle-encapsulated dye-sensitized core/Yb^{3+} shell UCNPs dispersed in PBS with and without 800 nm CW laser excitation obtained by an Apple iphone 5S camera.